

## Electronic Nature of Step-Edge Barriers against Adatom Descent on Transition-Metal Surfaces

Yina Mo,<sup>1</sup> Wenguang Zhu,<sup>2,3,\*</sup> Efthimios Kaxiras,<sup>1</sup> and Zhenyu Zhang<sup>3,2</sup>

<sup>1</sup>*Department of Physics and School of Engineering and Applied Sciences, Harvard University, Cambridge, Massachusetts 02138, USA*

<sup>2</sup>*Department of Physics and Astronomy, The University of Tennessee, Knoxville, Tennessee 37996, USA*

<sup>3</sup>*Materials Science and Technology Division, Oak Ridge National Laboratory, Oak Ridge, Tennessee 37831, USA*

(Received 12 December 2007; published 20 November 2008)

By studying a series of adatoms on representative transition-metal surfaces through first-principles calculations, we establish a clear correlation between the preferred mechanism and activation energy for adatom descent at a step and the relative degree of electronic shell filling of the adatom and the substrate. We also find an approximate linear relation between the adatom step-edge hopping barriers and the adatom-surface bonding strength with slope roughly proportional to the number of the adatom's nearest neighbors initially. These results may serve as simple guiding rules for predicting precise atomic surface morphologies in heteroepitaxial growth, as in formation of nanowires.

DOI: 10.1103/PhysRevLett.101.216101

PACS numbers: 68.35.Fx, 68.43.Bc, 68.43.Jk

In nanoscience, epitaxial growth continues to attract great interest as a powerful technique for producing low-dimensional structures with desirable properties [1–3]. A variation on the general theme of epitaxy is the formation of self-assembled nanowires at step edges where strikingly self-regulated growth has been observed [4–8]. These nanowires, composed of atoms different than the substrate (heteroepitaxy), represent an attractive realization of the long sought one-dimensional, atom-wide structures, that can serve as template for fundamental studies of electronic and magnetic behavior in low-dimensional systems. A key physical quantity that controls the nature of such growth phenomena is the Ehrlich-Schwoebel (ES) barrier [9,10], defined by  $\epsilon_{ES} = \epsilon_{se} - \epsilon_t$  (see Fig. 1), where  $\epsilon_t$  is the activation energy for adatom diffusion on a terrace, and  $\epsilon_{se}$  is the activation energy for adatom descent across a step edge (see Fig. 1). A small or nonexistent ES barrier generally favors layer-by-layer growth of smooth films, while a large one favors three-dimensional growth of rough films. While these notions have been well established for homoepitaxial growth systems [11], a far more complex picture emerges in the case of heteroepitaxial nanowires.

Adatoms on surfaces can migrate from the upper to the lower side of a step through either a hopping or an exchange process [12,13] (see Fig. 1). The activation energy for adatom descent at the step edge is the lower of the two barriers. Accordingly, the ES barrier in different cases may originate from different processes. In *homo*-epitaxial growth, either process leads to the same surface morphology after the adatom has diffused from the upper to the lower edge of the step. In *hetero*-epitaxial growth, the two processes result in different configurations: the hopping process places the hetero-adatom at the lower edge of the step, protruding from the step [Fig. 1(b)]; in contrast, the exchange leaves the hetero-adatom inside the step edge and a substrate atom protrudes onto the lower edge of the step [Fig. 1(c)]. Therefore, the value of the ES barrier alone does not fully describe the relevant physical processes; the

mechanism for diffusion across the step edge must also be identified. Repeated hopping or exchange events may lead to either a row of atoms decorating the lower step edge (hopping process dominates) [8], or a wire embedded within the step (exchange process dominates) [14]. Both processes produce relatively stable, one-dimensional, atom-wide wires that are well suited for the study of low-dimensional physics, but may exhibit very different magnetic and electronic properties. Our present study further demonstrates that the embedded wires may also serve as the building components for more elegant magnetic nanostructures (such as wires of mixed elements). However, it has so far been impossible to predict from simple considerations which process would dominate for a given system and why.

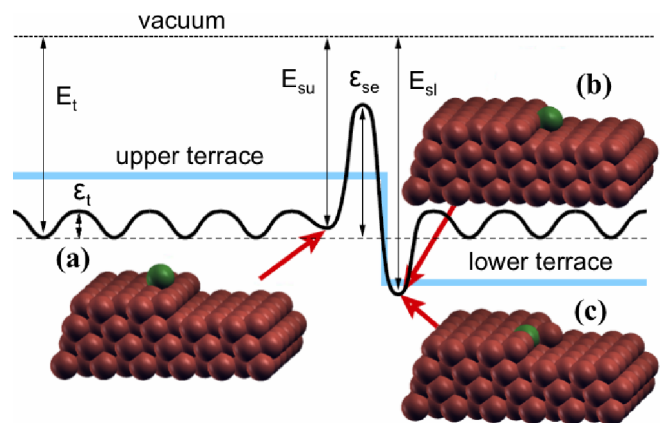


FIG. 1 (color online). Energetics and atomic structures for adatom (green sphere) motion across a surface step. (a) illustrates the initial configuration with the adatom at the upper edge of the step; (b) and (c) are the final configurations reached via direct adatom hopping or place exchange, respectively. The relevant binding energies ( $E_t$ ,  $E_{su}$ ,  $E_{sl}$ ) and energy barriers ( $\epsilon_{se}$ ,  $\epsilon_t$ ) are also indicated.

In this Letter, we study theoretically the electronic nature of ES barriers through systematic investigation of the energetics and kinetics of adatom interaction with the steps on metal surfaces. We consider two sets of adatoms on two representative stepped surfaces: Fe, Co, Cu, and Zn adatoms on a Cu(111) surface; and Rh, Pd, and Ag adatoms on a Pd(111) surface. Here we note that surface states are present on Cu(111), but are absent on Pd(111). Nevertheless, qualitatively similar trends are obtained for the adatom energetics and dynamics at the steps on both substrates in the present study, suggesting that these trends are mainly determined by the local electronic structures at the steps. On the other hand, the adatoms in each case are elements in the same row of the periodic table as the substrate atoms, thus of similar ionic sizes, thereby with minimal strain effects. Such systems are designed to expose potential electronic effects as in simple, idealized models (such as the jellium model), yet at the same time are physically realistic, some of which are being explored experimentally.

We find that the ES barriers are only slightly different from the corresponding step-edge barriers, because the terrace diffusion barriers for all the systems considered are much smaller than the step-edge barriers. We also find that the step-edge barriers display simple trends and are correlated with the electronic structure of the adatoms relative to the substrate atoms. We further show that the energy barrier for an adatom across a step edge via direct hopping scales approximately linearly with the adatom binding energy on the terrace and the slope of the linear function is roughly proportional to the number of the nearest neighbors of the adatom at the initial state. These results serve as a set of useful guiding rules in the design and control of self-assembled nanostructures on surfaces.

Our study is based on first-principles calculations in the context of density functional theory, employing VASP [15] with the generalized gradient approximation (PW91-GGA) [16] for exchange-correlation effects and ultrasoft pseudopotentials to represent the atomic cores [17]. Default plane-wave cutoffs from the GGA ultrasoft-pseudopotential database are used in the calculations, specifically, 233.729 eV and 199.020 eV for Cu and Pd, respectively. The Fermi-level smearing approach of Methfessel and Paxton [18] is used for the electronic states near the Fermi level, with a Gaussian width of 0.2 eV. Optimized atomic geometries are achieved when forces on all the unconstrained atoms are smaller in magnitude than 0.01 eV/Å. The bulk Cu and Pd lattice constants determined with these computational parameters are 3.64 and 3.96 Å, respectively, which compare well with the experimental values of 3.63 and 3.89 Å. In searching for the transition state, we use the “climbing image nudged elastic band” method [19], followed by spline interpolation, to determine the diffusion pathways and energy barriers. Typically four slab replicas between the initial and final geometries are enough to produce a smooth minimum energy path.

The stepped surfaces were modeled by a slab miscut along the (322) direction, consisting of (111) terraces that

are five atomic rows wide and separated by {100} faceted steps of monatomic height [20]. Trends at {111} faceted steps are expected to be similar. The supercell contains four atomic rows along the step direction and six layers with a total of 120 Cu or Pd atoms, separated by a vacuum region equivalent to 11.5 Å. The bottom three layers are fixed at their respective bulk positions during the relaxation. The Brillouin zone is sampled using a  $2 \times 2 \times 1$  mesh in the reciprocal space. We checked convergence by repeating the calculations for Fe adatoms on the stepped Cu (111) surfaces with a nine-layer slab and a  $3 \times 3 \times 1$  reciprocal space mesh; the results are well converged already in the six-layer slab calculations.

We start by discussing the adsorption energetics. The preferred adsorption sites of the adatoms on the stepped Cu (111) and Pd(111) surfaces are the fcc sites, whether they are in the central region of the terrace or in the immediate vicinity of the step. The difference between the fcc and hcp sites in the adsorption energy is typically less than 0.1 eV. With configuration (a) shown in Fig. 1 as the reference state, the energy of configurations (b) to (c) for the various systems considered, and the corresponding hopping and exchange barriers, are presented in Fig. 2.

Several distinctive trends emerge from these results. (i) For all the adatoms on Cu(111) or Pd(111), configurations (b) to (c) always have lower energies than (a). (ii) On each substrate, the binding strengths of both  $E_b$  and  $E_c$  decrease with increasing atomic number of the adatom (left to right in Fig. 2, lower panel). (iii) For adatoms to the left of the substrate element,  $E_c < E_b$ , indicating that (c) is the more stable configuration; in contrast, for adatoms to the

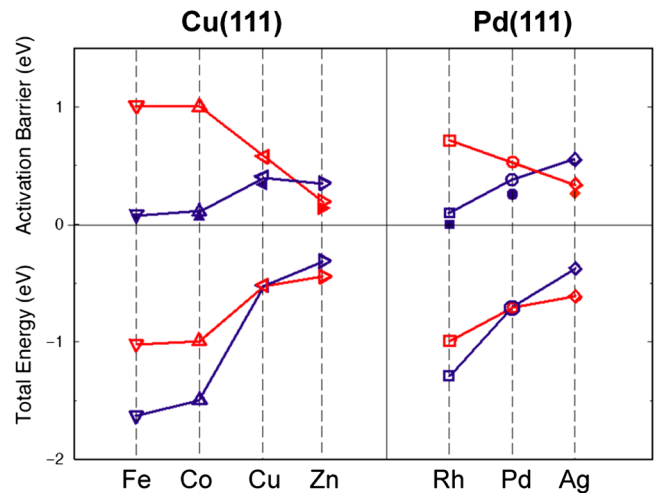


FIG. 2 (color online). Upper panel: Activation barriers  $\epsilon_{\text{hop}}$  for an adatom hopping from configuration (a) shown in Fig. 1 to (b) (red open symbols), and  $\epsilon_{\text{ex}}$  for adatom exchange from (a) to (c) (blue open symbols). The filled symbols are the corresponding ES barriers in each case, defined by the lower value between the hopping or exchange barriers minus the terrace diffusion barrier. Lower panel: Adatom adsorption energies  $E_b$  of configuration (b) (red), and  $E_c$  of configuration (c) (blue), both measured relative to that of (a).

right of the substrate element,  $E_b < E_c$ , with (b) being the more stable configuration. (iv) For both substrates, the direct hopping barriers from (a) to (b) ( $\epsilon_{\text{hop}}$ ) decrease with increasing atomic number of the adatom, while the exchange barriers from (a) to (c) ( $\epsilon_{\text{ex}}$ ) increase. (v) For adatoms to the left of (and including) the substrate element,  $\epsilon_{\text{ex}} < \epsilon_{\text{hop}}$ , namely, the exchange process is preferred; for adatoms to the right of the substrate element, direct hopping is preferred. (vi) The values of the ES barriers,  $\epsilon_{\text{ES}}$ , are all relatively small (less than 0.5 eV).

To elucidate the origin of the trends revealed above, we analyze the electronic interactions between the adatoms and the substrates by examining charge redistribution effects that describe the adatom-substrate binding strength. This is measured by the charge density difference between the system with the adatom, and that consisting of the substrate alone (with the same structure as when the adatom is present) plus the isolated adatom. The results are shown in Fig. 3, on the plane that is parallel to the step and contains the adatom and two nearest-neighbor substrate atoms, as depicted in the inset of Fig. 3. As is evident from this figure, electronic charge accumulates between the adatom and its nearest-neighbor substrate atoms, indicating formation of chemical bonds (in a general sense) between these atoms. The strength of these bonds, described by the charge redistribution, follows the same trend as the energy barriers for hopping. This correlation is physically sensible, because hopping down from the upper to the lower edge of the step involves breaking of the bonds. The stronger the bonds, the greater the energy cost to break them, or equivalently, the higher the potential energy barriers for direct hopping.

The trend in bonding strength revealed by the charge redistribution analysis can also be used to interpret the trends in the adsorption energies and exchange barriers. An adatom should prefer the embedded configuration

(c) when its bonding to the substrate atoms is strong, but should favor configuration (b) when the bonding is weak. This is consistent with the relative adsorption energies obtained: For adatoms to the left of the substrate element, which show strong bonding to the substrate atoms,  $E_c < E_b$ , while for adatoms to the right of the substrate element, which show weaker bonding,  $E_b < E_c$ . Note that for adatom self-diffusion,  $E_b = E_c$  by definition. Overall, the exchange barrier for adatoms that are strongly bonded to the substrate atoms should be smaller than that for adatoms that are weakly bonded, because the exchange process involves preserving the adatom-substrate bonds and breaking the bonds between the substrate atoms. Similarly, the hopping process should show opposite trends relative to the exchange process according to the variations in the adatom-substrate bond strength. These qualitative features are indeed confirmed quantitatively in Fig. 3. This qualitative picture of the hopping and exchange barriers is consistent with a simplified bond counting approach [21], but here emerges from a detailed analysis of first-principles electronic structure calculations rather than from empirical considerations.

Additional insight can be gained from the correlation between the adatom hopping barriers at step edges and the adatom binding energies on terraces. For each adatom-substrate combination, we consider the hopping barriers for both descending and ascending processes. The results are shown in Fig. 4. In all cases, the activation energy for hopping scales with the terrace binding energy, and to a reasonable approximation the relation is linear, consistent with the preceding analysis based on the adatom-substrate bonding strength. Besides the linear relationship, another intriguing aspect is the slope, which is roughly the same for both substrates (for a given process of descending or ascending, all the data points are approximately captured by the same line). Similar linear relationships were found

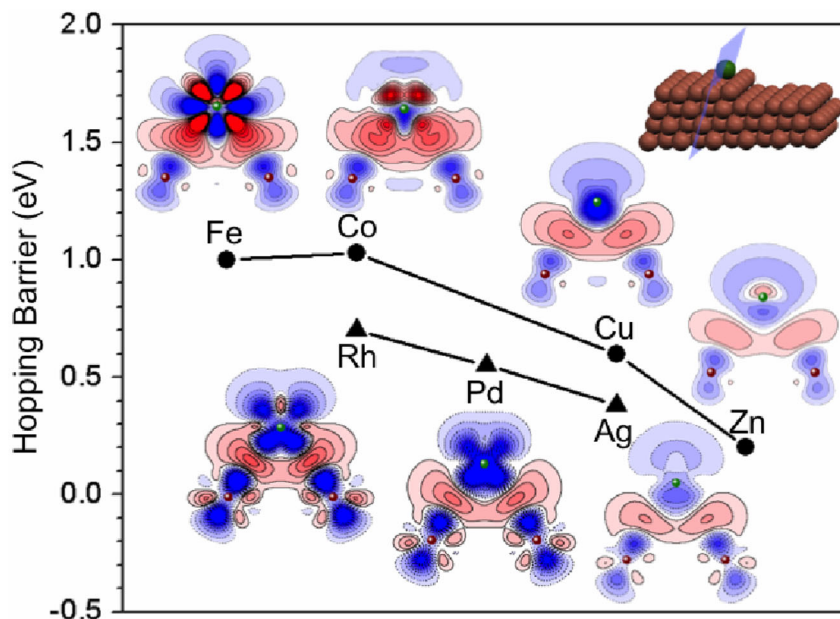


FIG. 3 (color online). Contour plots of charge redistribution of an adatom on Cu (111) (upper curve and contours) and Pd (111) (lower) in the plane depicted in the inset. Red and blue contours correspond to accumulation and depletion of electronic charge, respectively. The data points indicate the activation barriers for direct hopping.

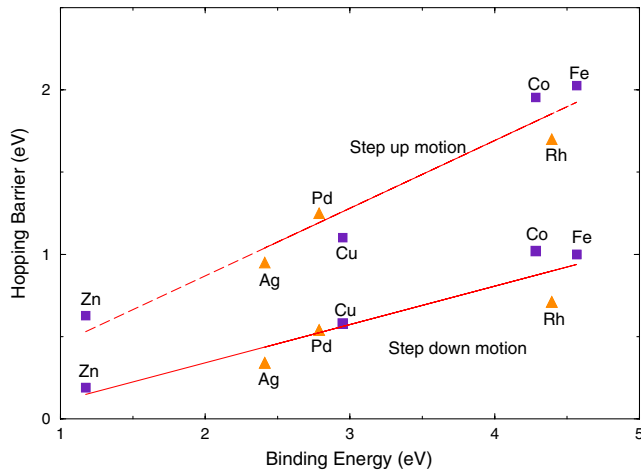


FIG. 4 (color online). Potential energy barriers against direct adatom hopping, ascending (upper) or descending (lower) a step, versus the adatom binding energies on terraces. The lines are linear fits to the calculated values (points). The purple square and orange triangle symbols represent different processes on Cu(111) and Pd(111), respectively.

for terrace diffusion of nonmetallic adatoms and molecules on transition-metal surfaces [22], but for the present systems, no such relationship exists between the terrace diffusion barriers and the binding energies, probably because the terrace diffusion barriers are too small on the close packed (111) surfaces. In addition, the slopes of the linear functions are roughly proportional to the number of the nearest neighbors of the adatom at the initial state. For the step-up line and the step-down line, the ratio between the slope (0.43 and 0.24, respectively) and the number of the adatom's nearest neighbors (5 at the lower step site and 3 at the upper step site) is 0.086 and 0.080, respectively.

The linear relations displayed in Fig. 4 cannot be extrapolated to adatom elements that are too far away from the substrate elements in the periodic table, especially if the adatoms and substrates belong to different rows in the periodic table. For example, calculations of the activation energies for W, Al, and Ga adatoms on the same stepped Cu(111) substrate show that these elements do not obey the simple linear relation defined by the Fe, Co, Cu and Zn adatoms. This is not surprising, because for elements that are distant from the substrate element, effects of different nature than the electronic effects considered above, such as strain, can play an important role.

One direct application of the present study is to facilitate controlled fabrication of low-dimensional nanostructures on stepped surfaces. For a given adatom-substrate system, one can estimate the step-edge hopping barrier from the adatom-terrace binding energy, which can be experimentally measured, and consequently predict the preferred kinetic process of the adatom at the step edge. Systems of similar nature should fit in the picture depicted in Fig. 4.

When generalized to situations involving more adatoms approaching a train of steps, nanowires decorating the steps, either at the lower step edges (resulting from direct hopping) or embedded in the steps (from exchange), will likely be formed. In fact, Fe embedded wires on a vicinal Cu(111) surface, belonging to the latter category, have recently been realized experimentally [14]. Such substrates, containing single-atom wires at their steps, may serve as templates for growing alloy wires when a third element is deposited subsequently.

This work was supported in part by DOE (CMSN Grant No. DE-FG02-05ER46226 and No. DE-FG02-05ER46209, and the Division of Materials Sciences and Engineering, Office of Basic Energy Sciences, DOE, under Contract No. DE-AC05-00OR22725 with Oak Ridge National Laboratory, managed by UT-Battelle, LLC), and by NSF (Grant No. DMR-0606485). The calculations were performed at NCCS of ORNL and NERSC of DOE.

\*wzhu3@utk.edu

- [1] Z. Y. Zhang and M. G. Lagally, *Science* **276**, 377 (1997).
- [2] H. Brune, *Surf. Sci. Rep.* **31**, 125 (1998).
- [3] O. Pietzsch, A. Kubetzka, M. Bode, and R. Wiesendanger, *Phys. Rev. Lett.* **92**, 057202 (2004).
- [4] H. J. Elmers *et al.*, *Phys. Rev. Lett.* **73**, 898 (1994).
- [5] J. de la Figuera *et al.*, *Appl. Phys. Lett.* **66**, 1006 (1995).
- [6] J. Shen *et al.*, *Phys. Rev. B* **56**, 2340 (1997).
- [7] V. Repain, J. M. Berroir, S. Rousset, and J. Lecoer, *Surf. Sci.* **447**, L152 (2000).
- [8] P. Gambardella, M. Blanc, L. Bürgi, K. Kuhnke, and K. Kern, *Surf. Sci.* **449**, 93 (2000).
- [9] R. L. Schwoebel and E. J. Shipsey, *J. Appl. Phys.* **37**, 3682 (1966).
- [10] G. Ehrlich and F. G. Hudda, *J. Chem. Phys.* **44**, 1039 (1966).
- [11] J. W. Evans, P. A. Thiel, and M. C. Bartelt, *Surf. Sci. Rep.* **61**, 1 (2006).
- [12] J. W. Evans, D. E. Sanders, P. A. Thiel, and A. E. DePristo, *Phys. Rev. B* **41**, 5410 (1990).
- [13] M. Villarba and H. Jónsson, *Phys. Rev. B* **49**, 2208 (1994).
- [14] J. Guo *et al.*, *Phys. Rev. B* **73**, 193405 (2006).
- [15] G. Kresse and J. Furthmüller, *Phys. Rev. B* **54**, 11 169 (1996).
- [16] J. P. Perdew and Y. Wang, *Phys. Rev. B* **45**, 13 244 (1992).
- [17] D. Vanderbilt, *Phys. Rev. B* **41**, 7892 (1990); G. Kresse and J. Hafner, *J. Phys. Condens. Matter* **6**, 8245 (1994).
- [18] M. Methfessel and A. T. Paxton, *Phys. Rev. B* **40**, 3616 (1989).
- [19] G. Henkelman, B. P. Uberuaga, and H. Jónsson, *J. Chem. Phys.* **113**, 9901 (2000).
- [20] R. Stumpf and M. Scheffler, *Phys. Rev. B* **53**, 4958 (1996).
- [21] M. Schroeder, P. Šmilauer, and D. E. Wolf, *Phys. Rev. B* **55**, 10 814 (1997).
- [22] A. U. Nilekar, J. Greeley, and M. Mavrikakis, *Angew. Chem., Int. Ed.* **45**, 7046 (2006).